The effect of short range correlation on the inelastic C2 and C4 form factors of ^{18}O nucleus

Adel K. Hamoudi, Abdullah S. Mdekil

Depatment of Physics, College of Science, University of Baghdad, Baghdad, Iraq

E-mail: physicsabdullah@yahoo.com

Abstract

The effect of short range correlations on the inelastic Coulomb form factors for excited 2^+ states (1.982, 3.919, 5.250 and 8.210MeV) and 4^+ states (3.553, 7.114, 8.960 and 10.310 MeV) in ^{18}O is analyzed. This effect (which depends on the correlation parameter β) is inserted into the ground state charge density distribution through the Jastrow type correlation function. The single particle harmonic oscillator wave function is used with an oscillator size parameter *b*. The parameters β and b are adjusted for each excited state separately so as to reproduce the experimental root mean square charge radius of ^{18}O. The nucleus ^{18}O is considered as an inert core of ^{12}C with two protons and four neutrons distributed over $1p_{1/2} - 1d_{5/2} - 2s_{1/2}$ active orbits. The total transition charge density comes from both the model space and core polarization transition charge densities. The realistic effective interaction of Reehal–Wildenthal (REWIL) is used for this model space. It is found that the introduction of the effect of short range correlations is necessary for obtaining a remarkable improvement for the calculated inelastic Coulomb form factors and considered as an essential for explanation the data amazingly throughout the whole range of considered momentum transfer.

Key words

Charge density distribution, inelastic Coulomb form factors, short range correlation.

Article info.

Received: May. 2016
Accepted: May. 2016
Published: Dec. 2016

تاثير دالة ارتباط المدى القصيرعلى عوامل التشكل الكولومية C2 و C4 للاستطارة الغير مرنة لنواة الاوكسجين -18

عادل خلف حمودي، عبدالله سوادي مديخل

قسم الفيزياء، كلية العلوم، جامعة بغداد، بغداد، العراق

الخلاصة

تمت دراسة تاثيردالة ارتباط المدى القصير على عوامل التشكل الكولومي غير المرن للحالات المتهيجة 2^+ ذوات الطاقات 1.982, 3.919, 5.250, 8.210 MeV و للحالات المتهيجة 4^+ ذوات الطاقات 8.960, 3.553, 7.114, 10.310 MeV. تم ادخال هذا التأثير (الذي يعتمد على مَعْلَمْ الارتباط β) على توزيع كثافة الشحنة للحالة الأرضية من خلال دالة الارتباط نوع Jastrow. تم استخدام الدالة الموجية للمتذبذب التوافقي للجسيم المنفرد مع مَعْلَمْ حجم التذبذب b. تم اعتبار β وb كمعلمات حرة تُغَير (لكل حالة متهيجة بصورة منفصلة) للحصول على النتائج العملية للجذر ألتربيعي لمعدل مربع نصف قطر الشحنة. أُفترِضَت النواة ^{18}O متكونة من قلب خامل ^{12}C مع بروتونين واربع بروتونات تتحرك في انموذج الفضاء $1p_{1/2}1d_{5/2}2s_{1/2}$. كثافة الشحنة الانتقالية الكلية تاتي من انموذج الفضاء وكثافة الشحنة الانتقالية لاستقطاب القلب. التفاعل المؤثر الواقعي لـ (Riwel) أُستعمل في انموذج الفضاء. لقد وُجِدَ ان إدخال تأثير دالة ارتباط المدى القصير يكون ضروري للحصول على تعديل ملحوظ وتحسين النتائج النظرية لعوامل التشكل الكولومية الغير المرنة كما ووُجد ايضا بانها أساسية لتفسير البيانات بشكل ممتاز خلال كامل مدى للزخم المنتقل المعتمد في هذه الدراسة.

Introduction

Electron scattering process can be explained according to the first Born approximation as an exchange of virtual photon, carrying a momentum, between the electron and the nucleus. The first Born approximation is being valid only if $Z\alpha << 1$, where Z is the atomic number and α is a fine structure constant. According to this approximation two types of electron scattering from the nucleus are recognized [1]. The first is the longitudinal or Coulomb scattering in which the electron interacts with the charge distribution of the nucleus where the interaction is considered as an exchange of a virtual photon carries a zero angular momentum along the direction of the momentum transfer*(q)*. This process gives all information about the nuclear charge distribution. In the second type, the electron interacts with the magnetization and current distributions and the process is considered as an exchange of a virtual photon with angular momentum ± 1 along q direction. This type of scattering is called transverse scattering and it provides the information about the nuclear current and magnetization distributions [2].

A simple phenomenological method for introducing dynamical short range and tensor correlations has been introduced by Dellagiacoma et al. [3]. The correlations are taken into account at small distances due to the hard- core nucleon- nucleon potential, which are not taken into account in the determinant form of the wave function of the system [2]. In that method a two–body correlation operator is introduced to act on the wave function of a pair of particles. It resembles the earlier approaches of constructing the exact wave function by means of an correlation operator [4] or by a correlation Jastrow [5] and Jastrow type [6, 7] factor which act on the uncorrelated determinant wave function. This method was proposed by Jastrow (1955) and was widely used with different modifications in many fields of physics concerned with Fermi systems [2].

In the studies of Massen et al. [8-10] an expression of the elastic charge form factor truncated at the two-body term, was derived using the factor cluster expansion of Clark and co-workers [11-13]. This expression, which is a sum of one- and two-body terms, depends on the harmonic oscillator parameter and the correlation parameter through a Jastrow-type correlation function [5]. This form is employed for the evaluation of the elastic charge form factors of closed shell nuclei ^{4}He, ^{16}O and ^{40}Ca. Subsequently, Massen and Moustakidis [14] performed a systematic study of the effect of the SRC on $s-p$ and $s-d$ shell nuclei. Explicit forms of elastic charge form factors and densities were found utilizing the factor cluster expansion of Clark and co-workers and Jastrow correlation functions which introduce the SRC. These forms depends on the single particle wave functions and not on the wave functions of the relative motion of two nucleons as was the case of our previous works [15-21] and other works [8,22,23].

It is important to point out that most of the previous studies were concerned with the analysis of the effect of the Short Range Correlations (SRC) on the elastic electron scattering charge form factors. In this work, the effect of SRC on the inelastic Coulomb form factors for excited 2^{+} (1.982, 3.919, 5.250 and 8.210 MeV) and 4^{+} states (3.553, 7.114, 8.960 and 10.310 MeV) in ^{18}O nucleus is studied. This effect is introduced in the ground state charge density distribution through the Jastrow type correlation function [5].

The nucleus ^{18}O is considered as an inert core of ^{12}C with two protons and four neutrons distributed over $1p_{1/2} - 1d_{5/2} - 2s_{1/2}$ active orbits. The interaction of REWIL [24] is used for this model space.

Theory

Inelastic electron scattering Coulomb form factor involves angular momentum J and momentum transfer q, and is given by [25]

$$\left|F_J^L(q)\right|^2 = \frac{4\pi}{Z^2(2J_i+1)}\left|\left\langle f \left\| \hat{T}_J^L(q) \right\| i \right\rangle\right|^2 \left|F_{cm}(q)\right|^2 \left|F_{fs}(q)\right|^2, \quad (1)$$

where $|i\rangle = |J_i T_i\rangle$ and $|f\rangle = |J_f T_f\rangle$ are the initial and final nuclear states (described by the shell model states of spin $J_{i/f}$ and isospin $T_{i/f}$), $\hat{T}_J^L(q)$ is the longitudinal electron scattering operator, $F_{cm}(q) = e^{q^2b^2/4A}$ is the center of mass correction (which removes the spurious states arising from the motion of the center of mass when shell model wave function is used), $F_{fs}(q) = e^{-0.43q^2/4}$ is the nucleon finite size correction and assumed to be the same for protons and neutrons, A is the nuclear mass number, Z is the atomic number and b is the harmonic oscillator size parameter.

The form factor of Eq.(1) is expressed via the matrix elements reduced in both angular momentum and isospin [26]

$$\left|F_J^L(q)\right|^2 = \frac{4\pi}{Z^2(2J_i+1)}\left|\sum_{T=0,1}(-1)^{T_f - T_{z_f}} \begin{pmatrix} T_f & T & T_i \\ -T_{z_f} & 0 & T_{z_i} \end{pmatrix} \left\langle J_f T_f \left\| \hat{T}_{JT}^L(q) \right\| J_i T_i \right\rangle\right|^2 \times \left|F_{cm}(q)\right|^2 \left|F_{fs}(q)\right|^2, \quad (2)$$

where in Eq. (2), the bracket ( ) is the three-J symbol, J and T are restricted by the following selection rules:

$$\left|J_f - J_i\right| \le T \le J_f + J_i$$
$$\left|T_f - T_i\right| \le T \le T_f + T_i, \quad (3)$$

and T_z is given by $T_z = \dfrac{Z-N}{2}$

The reduced matrix elements in spin and isospin space of the longitudinal operator between the final and initial many particles states of the system including configuration mixing are given in terms of the one-body density matrix (OBDM) elements times the single particle matrix elements of the longitudinal operator [27]

$$\left\langle f \left\| \hat{T}_{JT}^L \right\| i \right\rangle = \sum_{a,b} OBDM^{JT}(i, f, J, a, b) \left\langle b \left\| \hat{T}_{JT}^L \right\| a \right\rangle, \quad (4)$$

where a and b label single particle states (isospin included) for the shell model space. The OBDM in Eq. (4) is calculated in terms of the isospin-reduced matrix elements as [28]

$$OBDM(\tau_z) = (-1)^{T_f - T_Z} \begin{pmatrix} T_f & 0 & T_i \\ -T_z & 0 & T_z \end{pmatrix} \sqrt{2}\, \frac{OBDM(\Delta T = 0)}{2} + \tau_z (-1)^{T_f - T_Z} \begin{pmatrix} T_f & 1 & T_i \\ -T_z & 0 & T_z \end{pmatrix} \sqrt{6}\, \frac{OBDM(\Delta T = 1)}{2}, \quad (5)$$

where τ_z is the isospin operator of the single particle.

The model space matrix elements are not adequat to describe the absolute strength of the observed gamma-ray transition probabilities, because of the polarization in nature of the core protons by the model space protons and neutrons. Therfore the many particle reduced matrix elements of the longitudinal electron scattering operator $\hat{T}_J^L(q)$ is expressed as the sum of the model space (ms) contribution and the core polarization (cp) contribution [28], i.e.

$$\left\langle f \left\| \hat{T}_J^L(\tau_Z, q) \right\| i \right\rangle = \left\langle f \left\| \hat{T}_J^{ms}(\tau_Z, q) \right\| i \right\rangle + \left\langle f \left\| \hat{T}_J^{cp}(\tau_Z, q) \right\| i \right\rangle. \quad (6)$$

The model space matrix element, in Eq. (6), is given by

$$\left\langle f \left\| \hat{T}_J^{ms}(\tau_Z, q) \right\| i \right\rangle = \int_0^\infty dr\, r^2\, j_J(qr)\, \rho_{J,\tau_Z}^{ms}(i, f, r), \quad (7)$$

where $j_J(qr)$ is the spherical Bessel function and $\rho_{J,\tau_Z}^{ms}(i, f, r)$ is the model space transition charge density, expressed as the sum of the product of the OBDM times the single particle matrix elements, given by [28].

$$\rho_{J,\tau_Z}^{ms}(i, f, r) = \sum_{jj'(ms)}^{ms} OBDM(i, f, J, j, j', \tau_z)\, \left\langle j \| Y_J \| j' \right\rangle R_{nl}(r)\, R_{n'l'}(r). \quad (8)$$

Here, $R_{nl}(r)$ is the radial part of the harmonic oscillator wave function and Y_J is the spherical harmonic wave function.

The core-polarization matrix element, in Eq. (6), is given by

$$\left\langle f \left\| \hat{T}_J^{cp}(\tau_Z, q) \right\| i \right\rangle = \int_0^\infty dr\, r^2\, j_J(qr)\, \rho_{J,\tau_Z}^{cp}(i, f, r), \quad (9)$$

where $\rho_{J\tau_Z}^{cp}(i, f, r)$ is the core-polarization transition charge density which depends on the model used for core polarization. To take the core-polarization effects into consideration, the model space transition charge density is added to the core-polarization transition charge density that describes the collective modes of nuclei. The total transition charge density becomes

$$\rho_{J\tau_Z}(i, f, r) = \rho_{J\tau_Z}^{ms}(i, f, r) + \rho_{J\tau_Z}^{cp}(i, f, r) \quad (10)$$

According to the collective modes of nuclei, the core polarization transition charge density is assumed to have the form of Tassie shape [29]

$$\rho_{J t_Z}^{cp}(i, f, r) = N_T \frac{1}{2}(1 + \tau_z)\, r^{J-1} \frac{d\rho_{ch}^{gs}(i, f, r)}{dr}, \quad (11)$$

where N_T is the proportionality constant given by [15]

$$N_T = \frac{\int_0^\infty dr\, r^{J+2} \rho_{t_z}^{ms}(i,f,r) - \sqrt{(2J_i+1)B(CJ)}}{(2J+1)\int_0^\infty dr\, r^{2J} \rho_{ch}^{gs}(i,f,r)}, \quad (12)$$

which can be determined by adjusting the reduced transition probability $B(CJ)$ to the experimental value, and $\rho_{ch}^{gs}(i,f,r)$ is the ground state charge density distribution of considered nuclei.

For $N = Z$, the ground state charge densities $\rho_{ch}^{gs}(r)$ of closed shell nuclei may be related to the ground state point nucleon densities $\rho_p^{gs}(r)$ by [30, 31]

$$\rho_{ch}^{gs}(r) = \frac{1}{2}\rho_p^{gs}(r), \quad (13)$$

in unit of electronic charge per unit volume (e.fm^{-3}).

An expression of the correlated density $\rho_p^{gs}(r)$ (where the effect of the SRC's is included), consists of one- and two-body terms, is given by [14]

$$\rho_p^{gs}(r) \approx N_D\left[\left\langle \hat{O}_r \right\rangle_1 + \left\langle \hat{O}_r \right\rangle_2\right] \approx N_D\left[\left\langle \hat{O}_r \right\rangle_1 - 2O_{22}(r,\beta) + O_{22}(r,2\beta)\right], \quad (14)$$

where N_D is the normalization factor and $\hat{O}_r$ is the one body density operator given by

$$\hat{O}_r = \sum_{i=1}^{A} \hat{o}_r(i) = \sum_{i=1}^{A} \delta(\vec{r} - \vec{r}_i). \quad (15)$$

The correlated density $\rho_p^{gs}(r)$ of Eq.(14), which is truncated at the two-body term and originated by the factor cluster expansion of Clark and co-workers [11-13], depends on the correlation parameter β through the Jastrow-type correlation

$$f(r_{ij}) = 1 - \exp[-\beta(\vec{r}_i - \vec{r}_j)^2], \quad (16)$$

where $f(r_{ij})$ is a state-independent correlation function, which has the following properties: $f(r_{ij}) \to 1$ for large values of $r_{ij} = \left|\vec{r}_i - \vec{r}_j\right|$ and $f(r_{ij}) \to 0$ for $\vec{r}_{ij} \to 0$. It is so clear that the effect of SRC's, inserted by the function $f(r_{ij})$, becomes large for small values of SRC parameter β and vice versa.

The one-body term, in Eq. (14), is well known and given by

$$\left\langle \hat{O}_r \right\rangle_1 = \sum_{i=1}^{A} \left\langle i \left| \hat{o}_r(1) \right| i \right\rangle = 4\sum_{nl} \eta_{nl}(2l+1)\frac{1}{4\pi}\phi_{nl}^*(r)\phi_{nl}(r), \quad (17)$$

where η_{nl} is the occupation probability of the state nl and $\phi_{nl}(r)$ is the radial part of the single particle harmonic oscillator wave function.

The two-body term, in Eq. (14), is given by [14]

$$O_{22}(r,z) = 2\sum_{i<j}^{A} \left\langle ij \left| \hat{o}_r(1) g(r_1,r_2,z) \right| ij \right\rangle_a, \quad (z = \beta,\ 2\beta) \quad (18)$$

where

$$g(r_1,r_2,z) = \exp(-zr_1^2)\exp(-zr_2^2)\exp(2zr_1r_2\cos w_{12}), \quad (19)$$

The form of the two-body term $O_{22}(r,z)$ is then originated by expanding the factor $\exp(2zr_1r_2\cos w_{12})$ in the spherical harmonics and expressed as [14]

$$O_{22}(r,z) = 4\sum_{n_il_i,n_jl_j}\eta_{n_il_i}\eta_{n_jl_j}(2l_i+1)(2l_j+1) \times\left\{4A^{n_jl_jn_il_i0}_{n_il_in_jl_j}(r,z) - \sum_{k=0}^{l_i+l_j}\left\langle l_i0l_j0\middle|k0\right\rangle^2 A^{n_jl_jn_il_ik}_{n_il_in_jl_j}(r,z)\right\}, \quad (z=\beta,\,2\beta) \tag{20}$$

where

$$A^{n_3l_3n_4l_4k}_{n_1l_1n_2l_2}(r,z) = \frac{1}{4\pi}\phi^*_{n_1l_1}(r)\phi_{n_3l_3}(r)\exp(-zr^2) \times\int_0^\infty \phi^*_{n_2l_2}(r_2)\phi_{n_4l_4}(r_2)\exp(-zr_2^2)\; i_k(2zrr_2)r_2^2dr_2 \tag{21}$$

and $\left\langle l_i0l_j0\middle|k0\right\rangle$ is the Clebsch-Gordan coefficients.

It is important to point out that the expressions of Eqs. (17) and (20) are originated for closed shell nuclei with $N=Z$, where the occupation probability η_{nl} is 0 or 1. To extend the calculations for isotopes of closed shell nuclei, the correlated charge densities of these isotopes are characterized by the same expressions of Eqs. (17) and (20) (this is because all isotopic chain nuclei have the same atomic number Z) but this time different values for the parameters b and β are utilized.

The mean square charge radii of nuclei are defined by

$$\left\langle r^2\right\rangle = \frac{4\pi}{Z}\int_0^\infty \rho^{gs}_{ch}(r)\,r^4dr, \tag{22}$$

where the normalzation of the charge density distribution $\rho^{gs}_{ch}(r)$ is given by

$$Z = 4\pi\int_0^\infty \rho^{gs}_{ch}(r)\,r^2dr \tag{23}$$

Results and discussion

The effect of the SRC on the inelastic Coulomb form factors is studied for excited 2^+ states (1.982, 3.919, 5.250 and 8.210 MeV) and 4^+ states (3.553, 7.114, 8.960 and 10.310 MeV) in ^{18}O. Core polarization effects are taken into consideration by means of the Tassie model [Eq. (11)], where this model depends on the ground state charge density distribution. The proportionality constant N_T [Eq. (12)] is estimated by adjusting the reduced transition probability $B(CJ)$ to the experimental value. The effect of the SRC is incorporated into the ground state charge density distribution through the Jastrow type correlation function [5]. The single particle harmonic oscillator wave function is employed with an oscillator size parameter b.

The charge density distribution calculated without the effect of the SRC depends only on one free parameter (namely the parameter b), where b is chosen in such away so as to reproduce the experimental rms charge radius of ^{18}O. The charge density distribution calculated with the effect of the SRC depends on two free

parameters (namely the harmonic oscillator size parameter b and the correlation parameter β), where these parameters are adjusted for each excited state separately so as to reproduce the experimental rms charge radius of ^{18}O.

The nucleus of ^{18}O is assumed as a core of ^{12}C with 2 protons and 4 neutrons move in $1p_{1/2}$, $1d_{5/2}$ and $2s_{1/2}$ model space. In this model, the proton occupation probabilities in ^{18}O are assumed to be $\eta_{1s}=1$, $\eta_{1p}=0.95$, $\eta_{1d}=0.01$ and $\eta_{2s}=0.1$. Here, the total transition charge density [Eq. (10)] comes from both the model space and core polarization transition charge densities. The OBDM elements of ^{18}O are generated, via the shell model code OXBASH [32], using the REWIL [24] as a realistic effective interaction in the isospin formalism for 6 particles move in the $1p_{1/2}$, $1d_{5/2}$ and $2s_{1/2}$ model space with a ^{12}C core.

In Table 1, the experimental excitation energies E_x (MeV), experimental reduced transition probabilities $B(CL;0_1^+\rightarrow L^+)$ $(e^2\,\mathrm{fm}^{2L})$ and the chosen values for the parameters b and β for each excited state in ^{18}O are displayed. The root mean square (rms) charge radius with the effect of SRC is also displayed in this table and compared with that of experimental result. It is evident from this table that the values of the parameter b employed for calculations with the effect of SRC are smaller than that of without SRC ($b=1.8$ fm for ^{18}O). This is attributed to the fact that the introduction of SRC leads to enlarge the relative distance of the nucleons (i.e., the size of the nucleus) whereas the parameter b (which is proportional to the radius of the nucleus) should become smaller so as to reproduce the experimental rms charge radius of the ^{18}O.

Table 1: The experimental excitation energies and reduced transition probabilities, the chosen values for b and β as well as the rms charge radius calculated with the effect of the SRC of ^{18}O.

State	Ex (MeV)	$B(CL)$ $(e^2\,\mathrm{fm}^{2L})$	b (fm)	β (fm^{-2})	$<r^2>^{1/2}_{cal.}$ (fm)	$<r^2>^{1/2}_{\exp.}$ (fm)
2^+	1.982 [33]	44.8 ± 1.3 [33]	1.68	2.0	2.683	2.727 (20) [36]
2^+	3.919 [33]	22.2 ± 1.0 [33]	1.72	1.5	2.832	
2^+	5.250 [33]	28.3 ± 1.5 [33]	1.76	3.1	2.722	
2^+	8.210 [34]	7.3 ± 4.2 [34]	1.68	1.72	2.729	
4^+	3.553 [33]	$(9.04\pm0.90)\times10^2$ [33]	1.54	1.49	2.672	
4^+	7.114 [33]	$(1.31\pm0.06)\times10^4$ [33]	1.74	2.4	2.726	
4^+	8.96 [35]	$9.3(41)\times10^2$ [35]	1.51	1.55	2.620	
4^+	10.31 [35]	$<4\times10^2$ [35]	1.45	1.68	2.516	

The inelastic Coulomb form factors for different transitions ($J^\pi_{gs}T_{gs}\rightarrow J^\pi_f T_f$) in ^{18}O are displayed in Figs. 1-8. It is obvious that all transitions considered in these figures are of an isovector character. Besides, the parity of them

does not change. Here, the calculated inelastic form factors are plotted versus the momentum transfer q and compared with those of experimental data. The dashed and solid curves are the calculated inelastic Coloumb form factors without and with the inclusion of the effect of SRC, respectively. The open circles, open squares, closed circles and rhombic are those of experimental data taken from [33], [34] and [35].

In Fig. 1, the inelastic $C2$ form factors for the transition $0_1^+1 \rightarrow 2_1^+1$ ($E_x = 1.982$ MeV and $B(C2) = 44.8 \pm 1.3$ $e^2.\text{fm}^4$ [34]) are displayed. The calculated $C2$ form factors with the effect of the SRC are obtained using the values of $b = 1.68$ fm and $\beta = 2.0$ fm^{-2}. This figure illustrates that the calculated result displayed by the dashed curve (without the effect of the SRC) does not predict correctly the experimental data, where the diffraction minimum of this curve is not reproduced in the correct place of momentum transfer. Introducing the effect of the SRC leads to provide a notable modification in the calculated $C2$ form factors (displayed by the solid curve) and subsequently predicts the data amazingly throughout the whole range of considered momentum transfer.

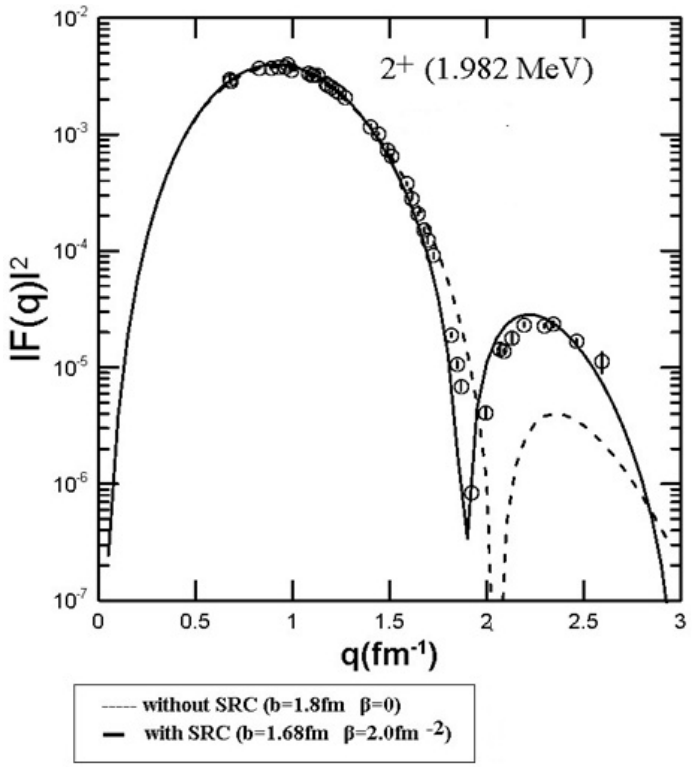

Fig. 1: Inelastic Coulomb $C2$ form factors for the transition to the 2^+1 (1.982 MeV) state. The dashed and solid curves are the calculated $C2$ form factors without and with the inclusion of the effect of the SRC, respectively. The open circle symbols are those of the experimental data taken from [33].

In Fig. 2 the inelastic Coulomb $C2$ form factors for the transition $0^+1 \rightarrow 2^+1$ ($E_x = 3.919$ MeV and $B(C2) = 22.2 \pm 1.0$ $e^2.\text{fm}^4$ [33]) are demonstrated. The calculated $C2$ form factors with the effect of the SRC are obtained using the values of $b = 1.72$ fm and $\beta = 1.5$ fm^{-2}. It is obvious from this figure that the calculated form

factors without the effect of the SRC (the dashed curve) disagrees clearly the data throught all range of considered *q*. Introduction the effect of the SRC leads to give a remarkable improvement in the calculated form factors (the solid curve) and then leads to describe the data amazingly for all range of momentum transfer. The rms charge radius evaluated by utilizing the above values of b and β is 2.832 fm, which is larger than the experimental value by 0.105 fm, which corresponds to an increase of approximately 3.85 % of the experimental value.

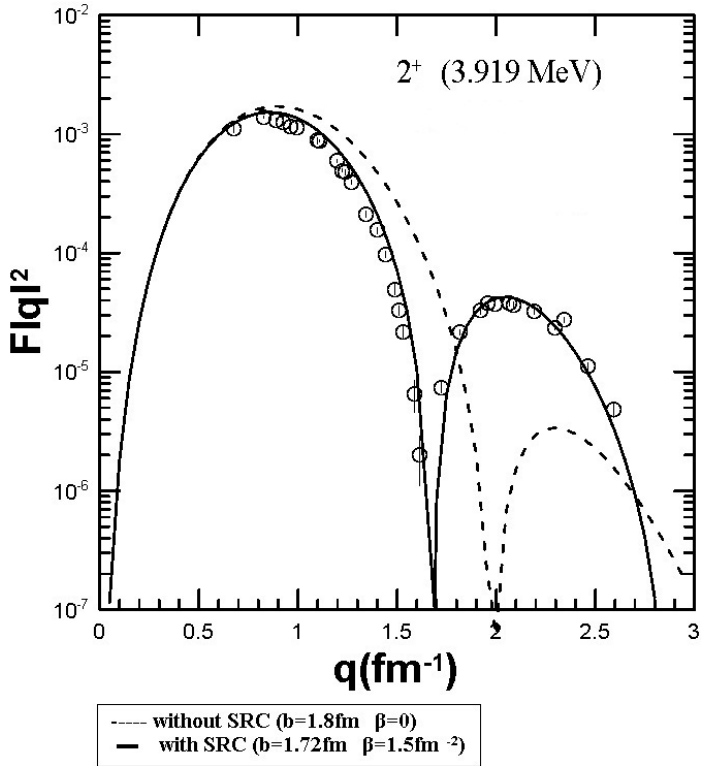

Fig. 2: Inelastic Coulomb $C2$ ***form factors for the transition to the*** 2^+1 ***(3.919 MeV) state. The dashed and solid curves are the calculated*** $C2$ ***form factors without and with the inclusion of the effect of the SRC, respectively. The open circle symbols are those of the experimental data taken from [33].***

In Fig. 3, the inelastic Coulomb $C2$ form factors for the transition $0^+1 \rightarrow 2^+1$ ($E_x = 5.250$ MeV and $B(C2) = 28.3 \pm 1.5$ $e^2.\text{fm}^4$ [33]) are presented. The calculated $C2$ form factors with the effect of the SRC are obtained using the values of $b = 1.76$ fm and $\beta = 3.1$ fm^{-2}. It is clear that the dashed curve does not describe the data at q >1.8 fm^{-1}. The inclusion of the effect of SRC leads to enhance slightly the calculated $C2$ form factors (the solid curve) in the first maximum but overestimates these data in the region of q >1.8 fm^{-1}. The rms charge radius calculated with the above values of b and β is 2.722 fm as shown in Table 1, which is in good agreement with the experimental value.

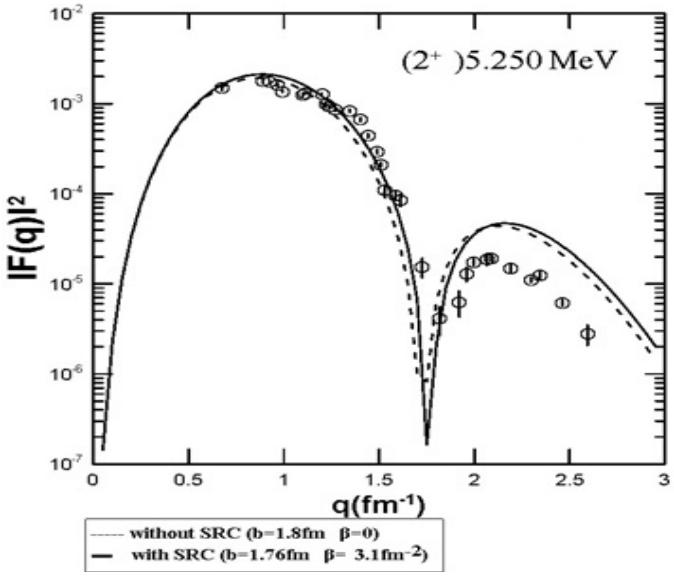

Fig. 3: Inelastic longitudinal $C2$ ***form factors for the transition to the*** 2^+1 ***(5.250 MeV) state. The dashed and solid curves are the calculated*** $C2$ ***form factors without and with the inclusion of the effect of the SRC, respectively. The open circle symbols are the experimental data taken from [33].***

In Fig. 4, the inelastic Coulomb $C2$ form factors for the transition $0^+1 \rightarrow 2^+1$ ($E_x = 8.210$ MeV and $B(C2) = 7.3 \pm 4.2$ $e^2.\text{fm}^4$ [34]) are exhibited. The calculated $C2$ form factors with the effect of the SRC are obtained using the values of $b = 1.68$ fm and $\beta = 1.72$ fm^{-2}. It is obvious that the dashed curve does not describes the data at $q \geq 1.8$. Inclusion the effect of SRC (solid curve) tend to enhance the calculated C2 form factors especially at the region of $q \geq 1.8$ fm^{-1} and consequently makes the results to be more closer to the data. Here the solid curve describes the experimental data extremely well for all momentum transfer considered.

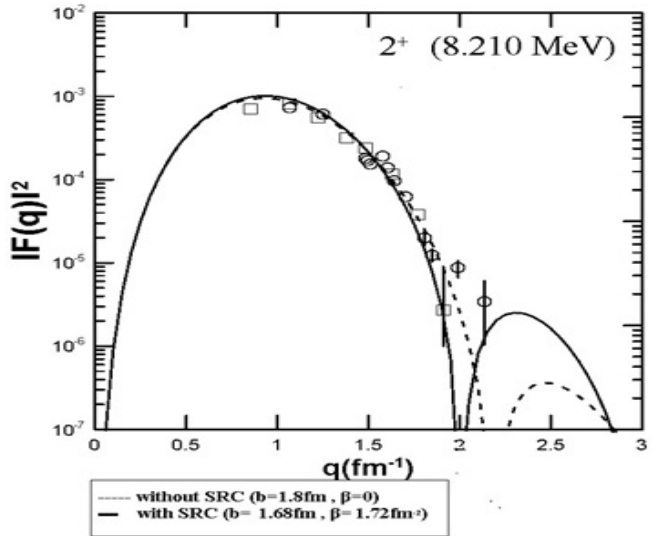

Fig. 4: The inelastic longitudinal $C2$ ***form factors for transition to the*** 2^+1 ***(8.210 MeV) state. The dashed and solid curves are the calculated*** $C2$ ***form factors without and with the inclusion of the effect of the SRC, respectively. The open square and open circle symbols are the experimental data taken from [34].***

In Fig. 5, the inelastic Coulomb $C4$ form factors for the transition $0^+1 \rightarrow 4^+1$ ($E_x = 3.553$ MeV and $B(C4) = (9.04 \pm 0.90) \times 10^2 \quad e^2.\text{fm}^8$ [33]) are displayed. The calculated $C4$ form factors (displayed by the solid curve) are obtained by adopting the values of $b = 1.54$ fm and $\beta = 1.49$ fm^{-2}. It is shown that the calculated C4 form factors without the effect of the SRC (the dashed curve) under predicts the experimental data throught all range of considered momentum transfer. Introduction the effect of the SRC improves the calculated C4 form factors appreciably and tends to describe the experimental data reasonably for all considered momentum transfer.

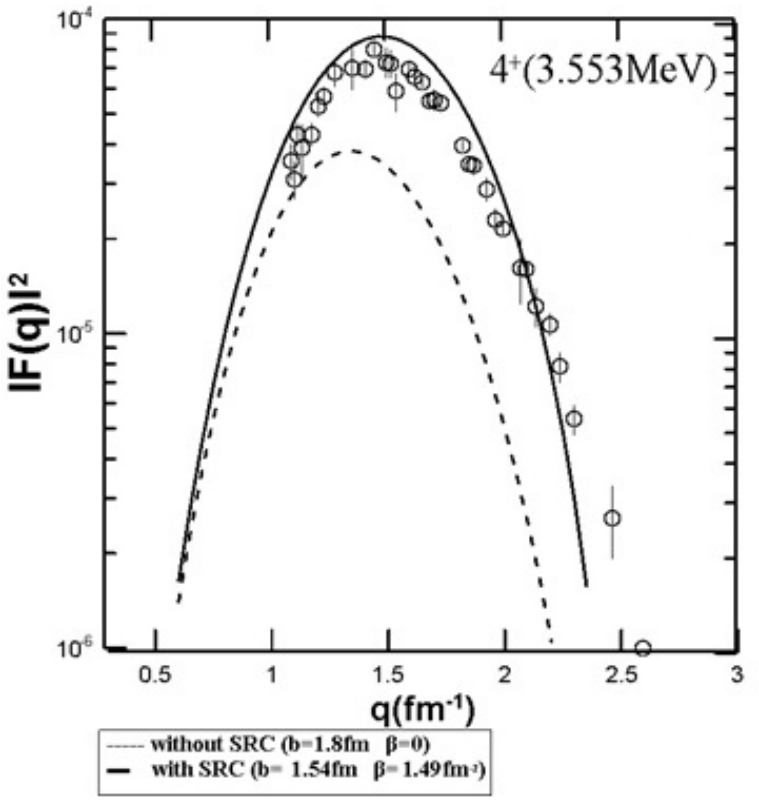

Fig. 5: Inelastic Coulomb $C4$ ***form factors for the transition to the*** 4^+1 ***(3.553 MeV) state. The dashed and solid curves are the calculated*** $C4$ ***form factors without and with the inclusion of the effect of the SRC, respectively. The open circle symbols are those of the experimental data taken from [33].***

In Fig. 6, the inelastic Coulomb $C4$ form factors for the transition $0^+1 \rightarrow 4^+1$ ($E_x = 7.114$ MeV and $B(C4) = (1.31 \pm 0.06) \times 10^4 \quad e^2.\text{fm}^8$ [33]) are exhibited. The calculated $C4$ form factors (displayed by the solid curve) are obtained by adopting the values of $b = 1.74$ fm and $\beta = 2.4\,\text{fm}^{-2}$. The calculated C4 form factors represented by the dashed and solid curves are in agreement with the experimental data. Inclusion the effect of SRC tends to improve slightly the calculated form factors as seen by the solid curve. In addition, the calculated rms charge radius is perfectly in agreement with the experimental value.

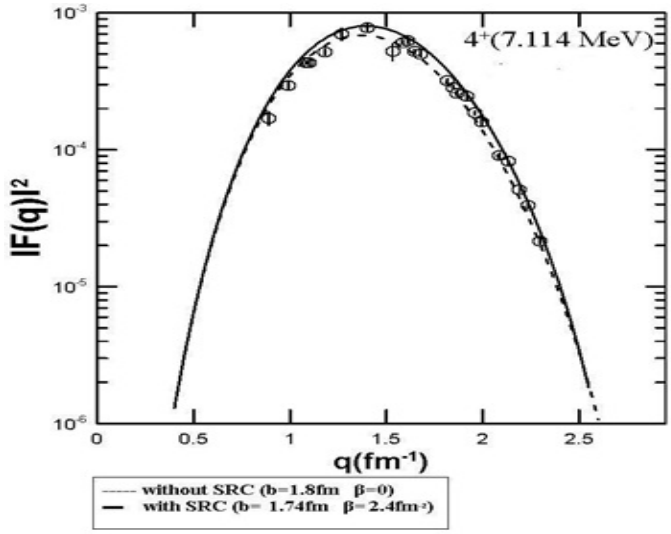

Fig. 6: Inelastic Coulomb $C4$ ***form factors for the transition to the*** 4^+1 ***(7.114 MeV) state. The dashed and solid curves are the calculated*** $C4$ ***form factors without and with the inclusion of the effect of the SRC, respectively. The open circle symbols are those of the experimental data taken from [33].***

In Fig. 7 the inelastic Coulomb $C4$ form factors for the transition $0^+1 \rightarrow 4^+1$ ($E_x = 8.96\,\text{MeV}$ and $B(C4) = 9.3(41)\times 10^2\ e^2.\text{fm}^8$[35]) are demonstrated. The calculated inelastic $C4$ form factors revealed by the solid curve (with the effect of the SRC) are obtained with applying the values of $b = 1.51$ fm and $\beta = 1.55$ fm^{-2}. It is clear from this figure that the calculated form factors without the effect of the SRC (the dashed curve) do not describe the experimental data very well. Inclusion the effect of the SRC leads to give a notable improvement in the calculated form factors (the solid curve) and then leads to describe the data amazingly.

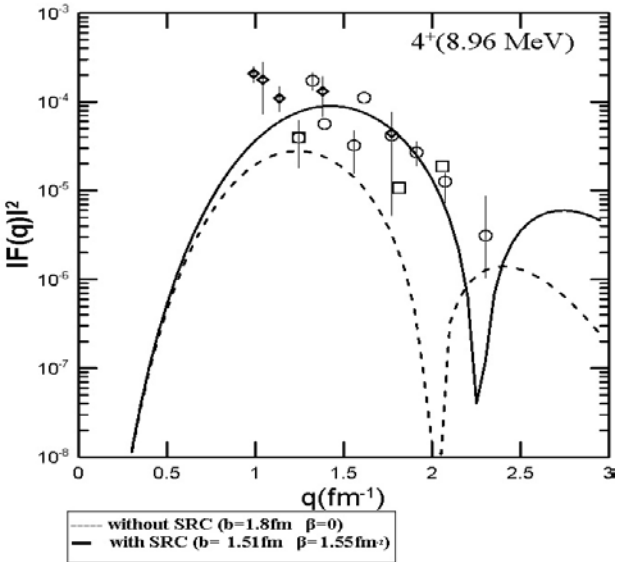

Fig. 7: Inelastic Coulomb $C4$ ***form factors for the transition to the*** 4^+1 ***(8.96 MeV) state. The dashed and solid curves are the calculated*** $C4$ ***form factors without and with the inclusion of the effect of the SRC, respectively. The open circle, open square and rhombic symbols are those of the experimental data taken from [35].***

In Fig. 8, the inelastic Coulomb $C4$ form factors for the transition $0^+1 \rightarrow 4^+1(E_x = 10.31$ MeV and $B(C4) =< 4\times10^2\ e^2.\text{fm}^8$ [35]) are presented. The calculated $C4$ form factors (the solid curve) are obtained by employing the values of $b = 1.45$ fm and $\beta = 1.68$ fm^{-2}. It is obvious that the dashed curve does not describe the data. Introduction the effect of the SRC (solid curve) leads to improve greatly the calculated form factors.

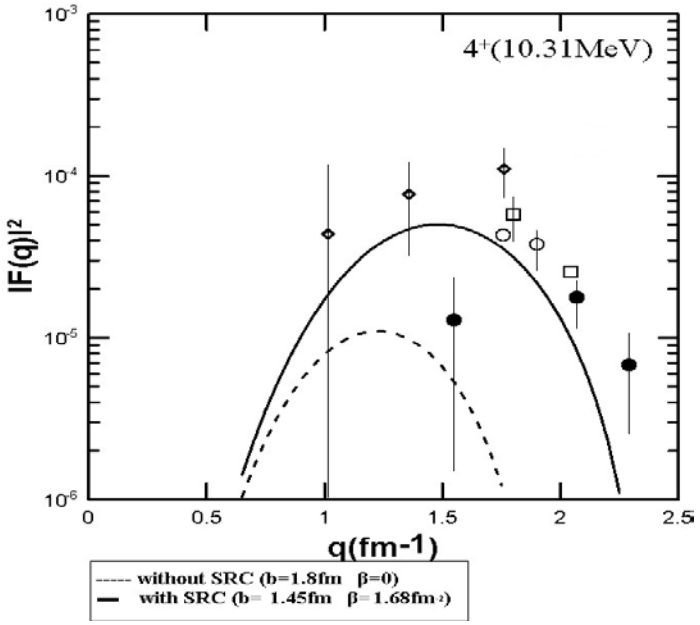

Fig. 8: Inelastic Coulomb $C4$ ***form factors for the transition to the*** 4^+1 ***(10.31 MeV) state. The dashed and solid curves are the calculated*** $C4$ ***form factors without and with the inclusion of the effect of the SRC, respectively. The open circle, closed circle, open square and rhombic symbols are those of the experimental data taken from [35].***

Conclusions

The effect of the SRC on the inelastic Coulomb form factors for the 2^+ states and 4^+ states in ^{18}O is analyzed. This effect is included in the present calculations through the Jastrow type correlation function. It is concluded that the introduction of the effect of the SRC is necessary for obtaining a notable modification in the calculated inelastic Coulomb form factors and also essential for explanation the data astonishingly throughout the whole range of considered momentum transfer.

References

[1] R. S. Willey, Nucl. Phys., A40, (1963) 529-565.
[2] A.N.Antonov, P.E. Hodgson, I.Zh. Petkov, Nucleon Momentum and Density Distribution in Nuclei, Clarendon Press, Oxford, (1988).
[3] F.Dellagiacoma, G.Orlandiniand, M.Traini., Nucl. Phys., A393 (1983) 95-108.
[4] K.A Brueckner., R.J. Eden, N.C. Francis, Phys. Rev., (1955) 98, 1445.
[5] R.Jastrow, 98, (1955)1497-184.
[6] G.Ripka, and J.Gillespie, Phys. Rev.Lett., 25 (1970) 1624-1625.
[7] S. Fantoni, and V.R. Pandharipande. Nucl. Phys., A427, (1984) 473-492.
[8] S.E.Massen, H.P. Nassena, C.P. Panos, J. phy., G 14(6), (1988) 753.
[9] S.E. Massen, and C.P.Panos, J.Phy., G 15, (1989) 311-319.

[10] S.E. Massen, J.phy., G 16(3), (1990) 1713.
[11] J.W. Clark and M.L. Ristig, Nuovo Cimento, A 70, (1970) 313-322.
[12] M.L.Ristig, W.J. Ter Low, J.W. Clark, Phys. Rev., C 3, 4 (1971) 1504-1513.
[13] J. W. Clark, Nucl. Phys., 2 (1979) 89 -199.
[14] S.E. Massen and Ch. C. Moustakidis, Phys. Rev., C 60 (1999) 24005.
[15] F.I. Sharrad, Ph.D Thesis. Department of Physics, College of Science, University of Baghdad, (2007).
[16] Gaith Naima Flaiyh, Ph.D Thesis. Department of Physics, College of Science, University of Baghdad, (2008).
[17] A. K.Hamoudi, R. A.Radhi, G. N. Flaiyh, F. I. Shrrad, Journal of Al-Nahrain University-Science, 13, 4 (2010) 88-98.
[18] A. K.Hamoudi, R. A. Radhi, G. N. Flaiyh, Engineering & Technology Journal, 28, 19 (2010) 5869-5880.
[19] A. K.Hamoudi, R. A. Radhi, G. N. Flaiyh, Iraqi J. Phys., 9, 14 (2011) 51-66.
[20] F. I.Sharrad, A. K.Hamoudi, R. A.Radhi, Y.Abdullah,Hewa, A. A. Okhunov, and H. Abu. Kassim, Chinese J. phys., 51, 3 (2013) 452-465.
[21] F. I.Sharrad, A. K.Hamoudi, R.Radhi, H. Y. Abdullah, Journal of the National Science Foundation of Sri Lanka, 41, 3 (2013) 209-217.
[22] Atti Ciofi degli, Nucl.Phys. A 129, (1969) 350.
[23] H.P. Nassena, J. Phys., G14 (1981) 927-936.
[24] McGrory, J. B. and Wildenthal, B. H., Phys. Rev., C 7 (1973) 974-993.
[25] Brown, B.A., Wildenthal,B.H. Williamson, C.F. Rad,F.N. Kowalski, S. Hall Crannell, O'Brien, J.T. Phys. Rev., C 32, 4 (1985) 1127-1156.
[26] T.W. Donnelly and I. Sick, Rev. Mod. Phys., 56, 3 (1984) 461-566.
[27] Brussard, P.J. and Glaudemans, P.W.M. Shell-model applications in nuclear spectroscopy, North Holland, Amsterdam (1977).
[28] B. A.Brown, A.R. Radhi, B.H. WildenthalPhys. Rep., 101, 5 (1983) 313-358.
[29] L.J. Tassie, Aust. J. Phys., 9, (1956) 407.
[30] A.K .Hamoudi, M.A. Hasan, and A.R. Ridha, Pramana J. phys., 78, 5 (2012) 737- 748.
[31] A. R. Ridha, M.Sc. Thesis. Department of Physics, College of Science, University of Baghdad, (2006).
[32] B.A.Brown, A.Etchegoyen, N.S. Godwin, W.D.M. Rae, W.A.Richter, W.E.Ormand, E.K.Warburton, J.S.Winfield, L.Zhao, C.H. Zimmerman, Oxbash for Windows, MSU-NSCL report number, 1289, (2005).
[33] B.E. Norum, M.V.Hynes, H.Miska, W.Bertozzi, J.Kelly, S.Kowalski, F.N. Rad, C.P. Sargent, T.Sasanuma, W.Turchinetz, Phys. Rev., C 25, 4 (1982) 1778-1800.
[34] D.M.Manlly, D.J.Millener, B.L. Berman, W.Bertozzi, T.N.Buti, J.M.Finn, F.W.Hersma, C.E.Hyde-Wright, M.V.Hynes, J.J.Kelly, M.A. Kovash, S.Kowalski, R.W.Louri, M.Murdock, B.E.Norum, B.Pugh, C.P. Sargent, Phys. Rev., C 41, 2 (1990) 448-457.
[35] R. M. Sellers, D. M. Manley, M.M.Niboh, D.S.Weerasundara, R. A. Lindgren, Causen, B. L., Farkhondeh, M., Norum, B.E. and Berman,B.L., Phys. Rev., C51 (1995) 1926-1944.
[36] H. De Vries, C.W. De Jager, C. De Vries, Atomic data and nuclear data tables, 36 (1987) 495.